AGU PUBLICATIONS

JGR

Journal of Geophysical Research: Biogeosciences

RESEARCH ARTICLE
10.1002/2017JG003836

Key Points:
- A 1°C increase in the Amazon's average daily maximum temperature could increase the number of active fires by 19 per Mha
- Relative to precipitation, temperature plays a more dominant role in regulating the number of active fires
- Concurrent drought and high temperatures substantially increase the likelihood of fires in the Amazon

Correspondence to:
C. H. R. Lima,
chrlima@unb.br

Citation:
Lima, C. H. R., AghaKouchak, A., & Randerson, J. T. (2018). Unraveling the role of temperature and rainfall on active fires in the Brazilian Amazon using a nonlinear Poisson model. *Journal of Geophysical Research: Biogeosciences*, *123*, 117–128. https://doi.org/10.1002/2017JG003836

Received 5 MAR 2017
Accepted 29 NOV 2017
Accepted article online 11 DEC 2017
Published online 15 JAN 2018

Unraveling the Role of Temperature and Rainfall on Active Fires in the Brazilian Amazon Using a Nonlinear Poisson Model

Carlos H. R. Lima[1], Amir AghaKouchak[2,3], and James T. Randerson[3]

[1]Department of Civil and Environmental Engineering, University of Brasilia, Brasilia, Brazil, [2]Department of Civil and Environmental Engineering, University of California, Irvine, CA, USA, [3]Department of Earth System Science, University of California, Irvine, CA, USA

Abstract Extreme droughts and high temperatures have become more frequent in the last two decades, increasing fire risk in the Amazon. The overarching goal of this study is to shed light on the influence of temperature and rainfall on fire occurrence for the 1998–2013 period. We use a Poisson regression to model satellite-based monthly fire counts across the Brazilian Amazon as a function of observed rainfall and temperature. Specifically, in the nonlinear regression framework we explore the fire count at month *t* as a function of the total monthly rainfall and monthly average of maximum daily temperatures at month *t* as well as lagged observations of these two predictors and of the fire counts. Our results indicate that the influence of temperature on fire counts can be larger than the effects of rainfall. Considering the temperature-fire relationship, the extra variance explained by rainfall is about 9%. Assuming average rainfall, we show that a 1°C increase in the monthly average of maximum daily temperatures results in a 30% increase in fire counts (19 fires per Mha more than the average), which translates into significant changes in the likelihood of fires within the Amazon. Our findings provide new insight about the role of temperature and rainfall in regulating fire occurrence in the Amazon, and the sensitivity of fire counts to relatively small changes in temperature highlights the vulnerability of the Amazon in a warming climate, where much higher temperatures are expected by the end of this century.

1. Introduction

The Amazon is the most extensive tropical rainforest in the world, supporting a high level of biodiversity and playing an essential role in global biosphere-atmosphere interactions. The dynamics of Amazon ecosystems exert considerable influence on biogeochemical cycles (McClain et al., 2001), moisture transport (Drumond et al., 2008), and regional climate of local and remote regions (Badger & Dirmeyer, 2016; Nobre et al., 1991). Extreme droughts in the Amazon seem to have become more frequent since 1995 (Marengo & Espinoza, 2016), and the drought magnitude has been positively associated with the number of active fires (Aragão et al., 2007; Brown et al., 2006; Chen et al., 2011; Ray et al., 2005), which release significant amounts of greenhouse gases and aerosols into the atmosphere (Artaxo et al., 2013; Cochrane, 2003; Gatti et al., 2014; Nepstad et al., 1999). The exceptional droughts of 2005 and 2010, for instance, deeply affected the Brazilian economy and caused an intensification of wild fires and associated impacts (Marengo et al., 2008, 2011; Phillips et al., 2009).

Droughts in the Amazon have been mainly associated with the El Niño–Southern Oscillation (ENSO) (Marengo & Espinoza, 2016) and the sea surface temperature (SST) variability in the tropical north Atlantic (Yoon & Zeng, 2010). Warm SST anomalies in the eastern tropical Pacific shift the descending branch of the Walker circulation over the Amazon and inhibit precipitation during the austral summer rainfall season (Ropelewski & Halpert, 1987; Sun et al., 2016). A warmer tropical north Atlantic will displace the Intertropical Convergence Zone to the north from its climatological position and therefore the ascending branch of the Hadley cell, which in turn reduce convection and precipitation over the Amazon. The fire season tends to occur between July and November in the southern Amazon, with a peak in September (Chen et al., 2013). An increase in the number of fires occurs during drought years (e.g., during 2005, 2007, and 2010). Statistical models have been developed to predict the fire season intensity in advance using SST anomalies in the tropical Atlantic and Pacific (Chen et al., 2011; Fernandes et al., 2011) as predictors, since it is believed that they are key variables in driving

rainfall anomalies in the region. Subsequent changes in terrestrial water storage influence transpiration and surface humidity during the following dry season (Chen et al., 2013; de Linage et al., 2014).

Fire dynamics in the Amazon arise from a complex interaction of climate, vegetation, and people (Aragão & Shimabukuro, 2010; Cochrane, 2003; Cochrane & Barber, 2009). Most fires in primary forest or disturbed vegetation cover types (logged areas, pasture, and crop fields) result from anthropogenic ignition sources, including intentionally ignited fires for forest clearing (deforestation), accidental fires, and those that escape out of control from agriculture or pasture maintenance (Cochrane, 2003; Nepstad et al., 1999). Deforested regions and pastures have also the potential to increase fire susceptibility in the Amazon and transform large areas of tropical forest into savanna or grass-dominated vegetation (Cochrane et al., 1999; Golding & Betts, 2008; Laurance & Williamson, 2001; Nepstad et al., 1999; Ray et al., 2005; Uhl & Kauffman, 1990; Veldman & Putz, 2011). Ecosystem composition regulates available fuels, with fire severity, intensity, and spread rate determined by a complicated interplay between ecosystems and climate. Intact closed-canopy Amazon forest provides a natural barrier for fire ignition and spread with high moisture content in the air and low radiation near the ground. The atmospheric moisture conditions are regulated by climate and modulated by ecosystems. During the wet season, groundwater is recharged by rainfall, supplying necessary water for the deep-root trees during the following dry season (Nepstad et al., 1999). Hence, humidity levels remain high during the dry season, which keeps the forest flammability relatively low during this period. In particular, the thin fuel layer on the forest ground continues to remain in equilibrium with high levels of surface humidity during the dry season. During severe droughts, the Amazon experiences an increase in the number of fires, which has been attributed to an increase in the forest susceptibility to fires due to a decline in the deep soil water storage and atmospheric moisture content in response to a persistent decrease in rainfall (Nepstad et al., 1999; Ray et al., 2005).

Here our work is motivated by the idea that climate-driven fire risk is primarily controlled by the deep and near surface soil water content, which in turn is driven by two main climate variables: rainfall, which directly replenishes groundwater levels, and temperature, which affects the water vapor deficit and evaporative demand in the atmosphere. Previous studies and fire models have linked the number of active fires to Amazon drought events and, ultimately, to ENSO and other climate models that influence rainfall in the Amazon by means of teleconnections (e.g., Alencar et al., 2006; Aragão et al., 2007; Brown et al., 2006; Cardoso et al., 2003; Fernandes et al., 2011; Roman-Cuesta et al., 2014; Turco et al., 2017; van der Werf et al., 2008). Some fire models (e.g., Nepstad et al., 1999, 2004; Silvestrini et al., 2011) take into account the effect of temperature indirectly through estimation of evapotranspiration, atmospheric evaporative demand, or water vapor pressure deficit. Several recent studies show that high temperatures exacerbate the effect of droughts (Aghakouchak et al., 2014; Swain et al., 2014; Shukla et al., 2015), leading to compounding effects of extremes (e.g., drought-high temperatures, Hao et al., 2013; Mazdiyasni & AghaKouchak, 2015). We therefore hypothesized that incorporation of the direct effects of temperature on the flammability of the Amazon forest deserves more attention. As we show through our analysis, droughts in the Amazon, as characterized by below average seasonal rainfall, are followed by a significant increase in the surface air temperature, which in turn could amplify the depletion of the deep soil water content. This would thus increase the climate-driven fire risk across the Amazon by contributing to ideal conditions for fire ignition and spread. Such scenarios of low rainfall and high temperatures may become more common in a warming climate and considerably extend the fire risk in the Amazon beyond existing projections (e.g., Cardoso et al., 2003; Liu et al., 2010; Silvestrini et al., 2011). Here we seek to improve our understanding of Amazon fires by quantifying the separate roles of temperature and rainfall in regulating the susceptibility of the Amazon forests to fire. We develop a nonhomogeneous, nonlinear Poisson regression model for the active fires in the Brazilian Amazon as a function of concurrent and past values of observed daily maximum temperature and rainfall. By evaluating the goodness of fit of different Poisson models as indicated by the R^2 measure, we explore the role of each of these variables in regulating forest flammability. After this introduction, this paper is organized as follows. The proposed Poisson model is described in section 2. The data are presented in section 3. Results are discussed in section 4, and finally, in section 5, we conclude by providing a summary of the main findings of this work.

2. Data

Satellite active fire observations for the Brazilian states within the Amazon region (Amazonas, Pará, Acre, Rondônia and Mato Grosso) are provided by the Brazilian National Institute of Space Research (INPE) Fire

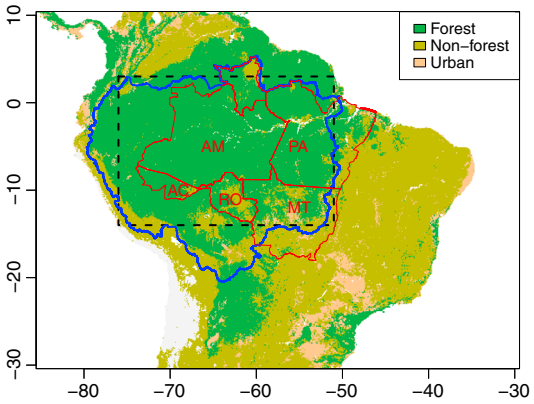

Figure 1. Grid domain (dashed line) of temperature and rainfall data over the Amazon watershed (blue line). The different land cover types follow the definition of NASA land cover maps available at http://eoimages.gsfc.nasa.gov/images/news/NasaNews/ReleaseImages/LCC/. The red line shows the political boundaries of the Brazilian federated states: Acre (AC), Amazonas (AM), Mato Grosso (MT), Pará (PA) and Rondônia (RO).

Monitoring Project. The data cover the period from June 1998 to May 2016 and can be obtained from http://www.inpe.br/queimadas/estatistica_estados. For the period June/1998 to June/2002 these fire data are based on NOAA-12 satellite, while from July/2002 through May/2016 fire observations are based on the AQUA satellite data. The difference between the NOAA-12 and AQUA satellite sensors were adjusted for by INPE in the fire product in order to keep a continuous pattern of fire detection and allow inferences on spatial and temporal trends in fire counts.

Monthly gridded (0.25° × 0.25°) temperature and rainfall data for the period 1980–2013 are provided by Xavier et al. (2016). These data consist of interpolated, daily rainfall and maximum daily temperature observations from 3,625 rainfall gauges and 735 weather stations across Brazil available from the National Institute of Meteorology, the National Water Agency, and the Department of Water and Electrical Energy of Sao Paulo. The interpolation schemes and validation procedures are described in Xavier et al. (2016). The geographical region delimited by the data set is shown in Figure 1. Here we use monthly values of rainfall and temperature that constitute, respectively, the sum of daily rainfall and the average of the maximum daily temperatures over each respective month. To avoid excessive noise in the data, we use the spatial average rainfall and temperature over the Amazon grid defined in Figure 1.

3. Methods

3.1. The Locfit Poisson Regression Model

Let us assume a variable Y_t that represents the number of active fires in the Brazilian Amazon (in the entire region or for a specific state) for month t. A common approach is to assume that Y_t follows a nonhomogeneous Poisson distribution with time varying rate λ_t

$$Y_t \sim \text{Pois}(\lambda_t), \tag{1}$$

where

$$\Pr(Y_t = k|\lambda_t) = \frac{e^{-\lambda_t}\lambda_t^k}{k!}. \tag{2}$$

The rate λ_t can be modeled as a function of predictors indexed by time t under the generalized linear model framework (McCullagh & Nelder, 1989):

$$\log(\lambda_t) = \alpha_0 + \alpha_1 \cdot P_t + \alpha_2 \cdot T_t, \tag{3}$$

where we adopt the canonical link function for λ_t, and P_t and T_t are the precipitation and temperature for month t, respectively.

In order to account for the fire counts relative to the area of the Amazon (or the respective states), we add the area A (in Mha) as an exposure (or offset) input, so that we essentially model the rate $\frac{\lambda_t}{A}$ as a function of the covariates:

$$\log(\lambda_t) = \log(A) + \alpha_0 + \alpha_1 \cdot P_t + \alpha_2 \cdot T_t. \tag{4}$$

Note that under this model, λ_t (or more precisely $\frac{\lambda_t}{A}$) changes exponentially as a function of P_t and T_t. In order to allow more complex relationships, we assume here a local regression model (locfit, see Loader, 1999 for more details) for $\log(\lambda_t)$

$$\log(\lambda_t) = f(\log(A)\,, P_t\,, T_t), \tag{5}$$

with $f(\cdot)$ being a smooth, polynomial function (linear or quadratic) fitted within a sliding window. For instance, a local linear model around a point $\mathbf{X} = (P, T)$ can be written as

$$\log(\lambda_t) \approx \log(A) + a_0 + a_1 \cdot (P_t - P) + a_2 \cdot (T_t - T), \tag{6}$$

where the coefficients a_0, a_1, a_2 are estimated, for each fitting point $\mathbf{X} = (P, T)$, using the weighted least squares

$$\sum_{t=1}^{n} W\left(\frac{\|\mathbf{X}_t - \mathbf{X}\|}{h}\right)\left(\log(\lambda_t) - (\log(A) + a_0 + a_1 \cdot (P_t - P) + a_2 \cdot (T_t - T))\right)^2, \tag{7}$$

with h being the bandwidth (i.e., smoothing parameter), $\|\cdot\|$ the Euclidean norm, n the total number of observations, and W the tricube weighting function:

$$W(u) = \begin{cases} (1 - |u|^3)^3, & |u| < 1 \\ 0, & \text{otherwise.} \end{cases} \tag{8}$$

More details can be seen in Loader (1999). The term $\log(A)$ remains as an offset in the model, and hereafter, we refer to this model with predictors P_t and T_t as the benchmark model. Subsequently, past values of observed fire counts (y_{t-1} , y_{t-2}, etc.), rainfall, and temperatures will also be added to the model for further evaluation.

We use the freely available *R* package locfit (Loader, 2013) for model fitting. We set the default values (as provided by the locfit package) for the model parameters: $\alpha = 0.7$ (nearest neighbor fraction, which gives a bandwidth covering 70% of the data), deg = 2 (degree of local polynomial), and the tricube weight function. We have used the same set of parameters across all models so that the models can be evaluated against each other (see section 4).

The Poisson model presented in equation (1) has the property that the expected value of Y_t ($E(Y_t) = \lambda_t$) is equal to its variance $\mathrm{Var}(Y_t)$. However, very often this is not the case and the variance of Y_t can be greater than its mean, which is known as overdispersion. Model (1) can still be used to estimate the expected number of fire counts $E(Y_t)$, but its variance can be severely underestimated. In this work we handle overdispersed data by assuming a quasi-likelihood model (Loader, 2013), in which the only change relative to the corresponding likelihood model will be in estimating the variance $\mathrm{Var}(Y_t)$:

$$\mathrm{Var}(Y_t) = \sigma^2 \cdot \lambda_t, \tag{9}$$

with σ^2 being the dispersion parameter. We refer the reader to Loader (2013) for the exact formulation to estimate σ^2 after fitting the Poisson model (equations (1) and (5).

3.2. Model Diagnostic and the Pseudo R^2 Measure for Poisson Regression

A common metric for diagnostic and comparison in generalized linear models is the deviance (McCullagh & Nelder, 1989), which can be defined for a single observation y_t as

$$d_t(y_t, \hat{\lambda}_t) = 2 \cdot \left(\sup_{\lambda} l(y_t, \lambda) - l(y_t, \hat{\lambda}_t)\right), \tag{10}$$

where $l(y_t, \hat{\lambda}_t)$ is the log likelihood of the fitted model for observation y_t and $\sup_\lambda l(y_t, \lambda)$ is the maximum log likelihood achievable in a full model with the number of parameters being equal to the number of observations. Hence, the deviance provides a measure of the difference between the maximum log likelihood achievable (i.e., a model that is a perfect fit to the data) and the log likelihood of the model under investigation.

The total deviance is given by the sum of d_t over all observations y_t, $t = 1, \ldots, n$:

$$D = \sum_{t=1}^{n} d_t(y_t, \hat{\lambda}_t) = \sum_{t=1}^{n} 2 \cdot \left(\sup_{\lambda} l(y_t, \lambda) - l(y_t, \hat{\lambda}_t)\right). \tag{11}$$

For the Poisson model adopted in this work, the total deviance is given by

$$D = 2 \sum_{t=1}^{n} \left[y_t \log\left(\frac{y_t}{\hat{\lambda}_t}\right) - (y_t - \hat{\lambda}_t)\right]. \tag{12}$$

Since we use the deviance statistic D as a measure of model discrepancy, the fitting diagnostic will be carried out by analyzing the deviance residuals (McCullagh & Nelder, 1989):

$$r_t = \mathrm{sign}(y_t - \hat{\lambda}_t)\sqrt{d_t}, \tag{13}$$

so that

$$\sum_{t=1}^{n} r_t^2 = D. \tag{14}$$

The goodness-of-fit analysis done in this work (not shown here) follows the procedures as recommended for standard linear regression models (QQ-plot, residuals versus predictor variables, serial plots, etc). However, the coefficient of determination R^2 as used in linear regression cannot be directly extended to the Poisson regression model, since residuals are no more homoscedastic. We use then the deviance D in equation (12) as a measure of goodness of fit for a given model and define the pseudo R^2 measure as

$$R^2 = 1 - \frac{D}{D_{\text{null}}}, \tag{15}$$

with D_{null} being the deviance of the Poisson regression model (i.e., null model) with just the offset and the intercept term α_0 in equation (4), so that the predicted mean is

$$\hat{\lambda}_t = \frac{1}{n}\sum_{t=1}^{n} y_t = \bar{y}\,, \tag{16}$$

and D_{null} becomes

$$D_{\text{null}} = 2\sum_{t=1}^{n}\left[y_t \log\left(\frac{y_t}{\bar{y}}\right) - (y_t - \bar{y})\right] = 2\sum_{t=1}^{n}\left[y_t \log\left(\frac{y_t}{\bar{y}}\right)\right]. \tag{17}$$

The pseudo R^2 measure can be viewed then as the gain in explained deviance by the proposed model over the null model with just an intercept term. R^2 ranges from 0 to 1, with 1 being a perfect fit. Cameron and Windmeijer (1996) present a comparison of different R^2 measures for Poisson regression models and suggest the use of R^2 based on the deviance residuals as adopted here.

The role of temperature and rainfall at month t on the same month fire (y_t) count across the Amazon will be explored here by analyzing changes in the R^2 measure as the deviance D in equation (15) varies by including and removing these predictors in equation (5). The effect of past temperature, rainfall, and fire count (e.g., y_{t-1}) will be assessed in a similar manner, but the predictors in equation (5) will be past values, such as T_{t-1} and P_{t-1}.

Finally, the conditional effect of past temperature and rainfall on the fire count at time t given the concurrent observations of rainfall P_t and temperature T_t will also be evaluated by replacing D_{null} with D_{bench}. The latter is calculated for the benchmark model in equation (5), which includes only P_t or T_t as predictors, with D adding an additional lagged variable (P, T, or the past fire count y) to the benchmark model. For instance, if we want to evaluate the conditional effect of the rainfall lagged by 3 months on the fire count at time t given that we know the rainfall and temperature at time t, we will look at the R^2 measure

$$R^2 = 1 - \frac{D_{p3}}{D_{\text{bench}}}, \tag{18}$$

where D_{p3} is the deviance estimated by the locfit Poisson regression model considering the predictors (P_t , T_t , P_{t-3}), and D_{bench} is the deviance estimated for the benchmark Poisson model with predictors (P_t , T_t).

Note that Y_t and A in equations (4) and (5) will change according to the state. For the entire Brazilian Amazon model, they will be the sum of the respective variables across the states Amazonas, Pará, Mato Grosso, Acre, and Rondônia. On the other hand, the predictors (P_t , T_t, etc.) are spatial averages over the Amazon region and thus change only over time, remaining the same as the model changes across states.

4. Results

4.1. Exploratory Analysis of Temperature and Rainfall Time Series

The observed series of monthly temperature (average of maximum daily temperatures over the respective month) averaged over the Amazon region as defined in Figure 1 displays a remarkable increasing trend (Figure 2a) of 0.03°C per year. The Mann-Kendall trend test rejects the null hypothesis of no monotonic trend in the temperature data (p value $< 2.2 \cdot 10^{-16}$). On the other hand, the monthly rainfall series (Figure 2b) does not

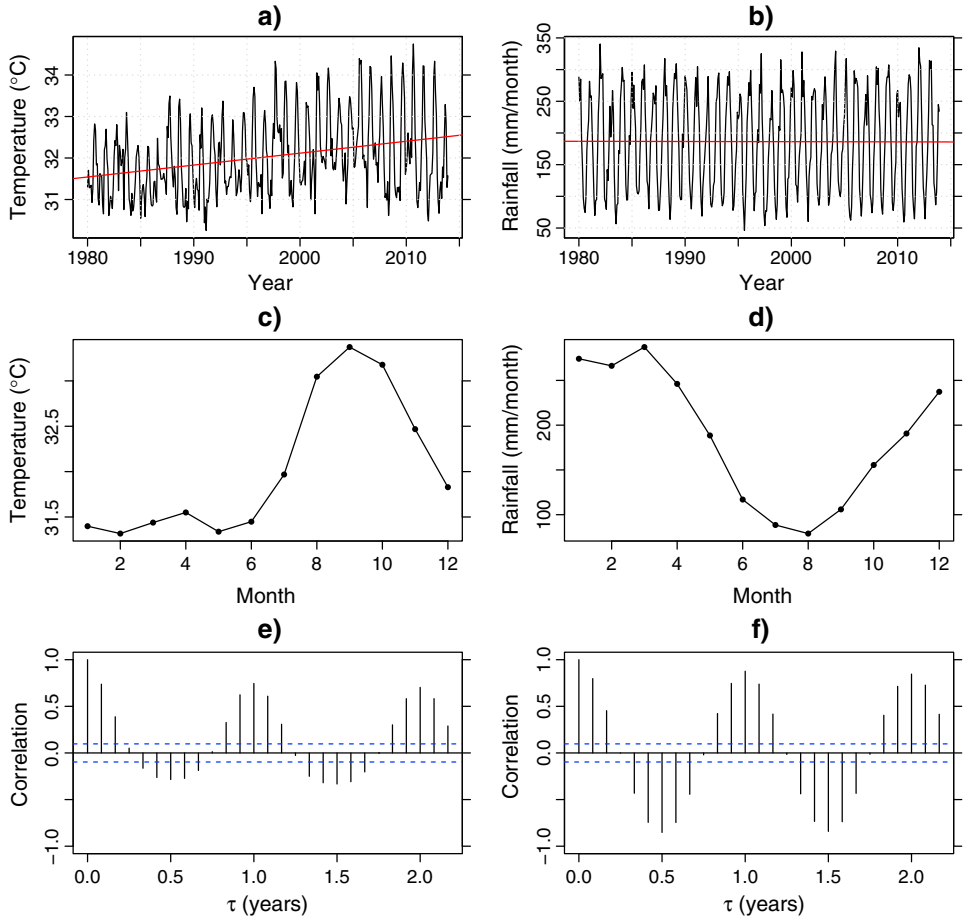

Figure 2. (a) Time series of spatially average temperature and (b) rainfall over the Amazon region as defined in Figure 1. Seasonal cycle of spatially average (c) temperature and (d) rainfall. Autocorrelation function of spatially average (e) temperature and (f) rainfall. The red line shows an ordinary linear regression fit to the data.

show any evidence of a significant trend in the last 30 years (Mann-Kendall test p value = 0.93). These results are consistent with previous studies (Malhi & Wright, 2004) that found no trend in rainfall over the Amazon. However, averaging rainfall across the grid points may have smoothed an apparent dipole trend of increasing/decreasing rainfall in the northern/southern Amazon detected in other studies (Debortoli et al., 2015; Rao et al., 2016). It is also worth mentioning that other studies (Fernandes et al., 2015; Gloor et al., 2015; Malhi & Wright, 2004) have also provided evidence of multidecadal variability in rainfall and temperature over the Amazon. For instance, temperature across the Amazon in the 1970s was cooler than previous decades, while the annual mean precipitation was generally higher than previous decades, coinciding with specific patterns in the SSTs at the Atlantic and Pacific Oceans as well as changes in the phase of the Pacific Decadal Oscillation. Such multidecadal changes may impact short-term, monotonic trends. Therefore, multidecadal and low-frequency variability should be considered when interpreting precipitation and temperature trends.

Both temperature and rainfall present a well-defined seasonal cycle (Figures 2c and 2d), but they are out of phase, with maximum (minimum) temperature in September (February) while the rainfall has its maximum (minimum) in March (August). The autocorrelation function (Figures 2e and 2f) shows a persistence of 2 months for both temperature and rainfall and peaks at around multiples of 6 months that reflect the well-defined seasonal cycle.

Monthly temperature and rainfall are strongly correlated (Figure 3a), with a Pearson correlation coefficient of −0.58. The null hypothesis of no linear relation between the two variables is rejected at the 5% significance level (p value $< 2.2 \cdot 10^{-16}$). In order to verify whether such relationship is driven by the seasonal cycle of rainfall and temperature, we remove from the original series the monthly mean values and obtain anomalies.

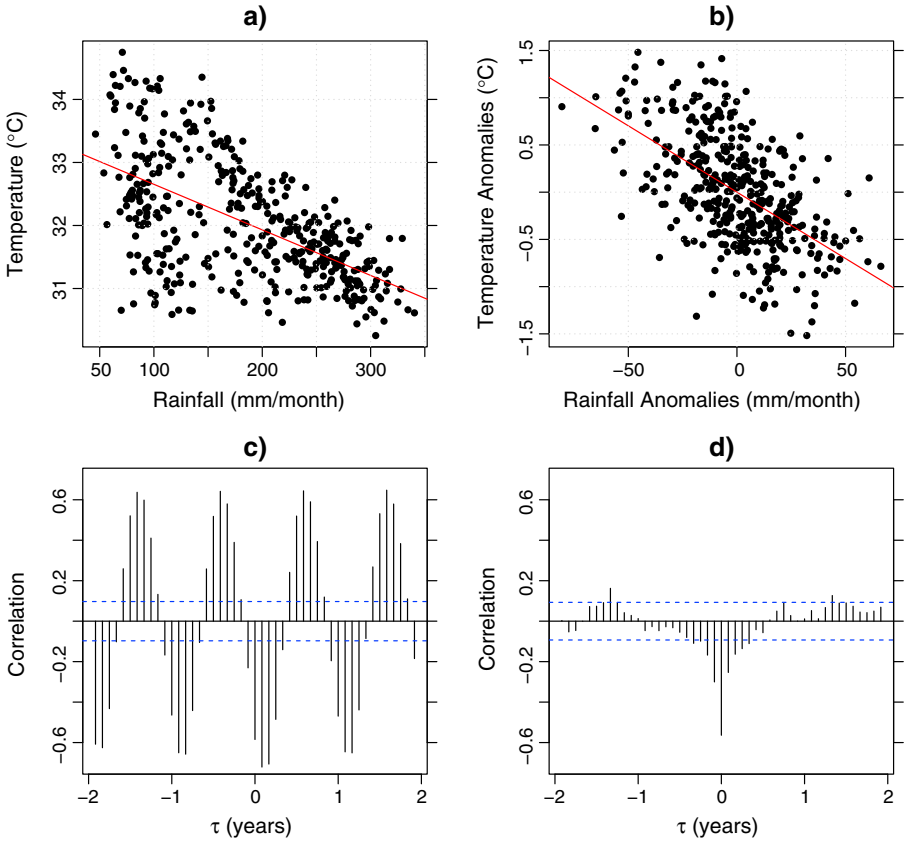

Figure 3. Scatterplot of temperature versus rainfall for the (a) raw data and for (b) anomalies obtained after removing the seasonal cycle. The red line shows an ordinary linear regression fit to the data. Correlation (cross-correlation function) of temperature ($t + \tau$) and rainfall (t) for the (c) raw data and for (d) anomalies obtained after removing the seasonal cycle.

The scatterplot of temperature versus rainfall after removing the seasonal cycle is shown in Figure 3b. The relationship remains strong, with a Pearson correlation coefficient of −0.38 and the null hypothesis is again rejected (p value = $1.423 \cdot 10^{-15}$).

At monthly scale, there is no evidence that the positive anomalies in temperature are a response of the vegetation to negative anomalies in rainfall or that positive temperature anomalies lead to a reduction in the Amazon rainfall. In fact, the cross-correlation function (Figures 3c and 3d) shows the out-of-phase seasonal cycle of rainfall and temperature in the raw data (Figure 3c) and a correlation between anomalies that peaks at lag zero (Figure 3d), possibly due to the short wave radiative effect of low cloudiness on the surface energy balance and consequently on the surface temperature. This suggests that both anomalies in rainfall and temperature are driven by the same mechanisms.

4.2. Exploratory Analysis of Fire Counts, Rainfall, and Temperature

The annual series of active fires (sum of monthly values and per Mha) for the Brazilian states within the Amazon region is displayed in Figure 4a. The period 1999–2005 is characterized by higher fire count than the later period, particularly for the states of Mato Grosso and Rondônia, which are by far the states with the largest number of fires. This is consistent with other studies (Chen et al., 2013) that found an increase in the number of active fires during the 2001–2005 period and attributed it mainly to deforestation. The seasonal cycle of fire count (Figure 4b) resembles the cycle of temperature, with a peak in August–September. This study ultimately seeks to better understand the reason for the fire count peak in August–September: is it due to the low rainfall, high temperatures, or both? if the latter, what is the role of each variable?

The scatterplot of the relationships between active fires over the Brazilian Amazon (sum of the fire counts of Amazonas, Mato Grosso, Rondônia, Para, and Acre states) and temperature and rainfall averaged over the grid defined above is displayed in Figure 5. A strong nonlinear relationship with fire counts can be observed

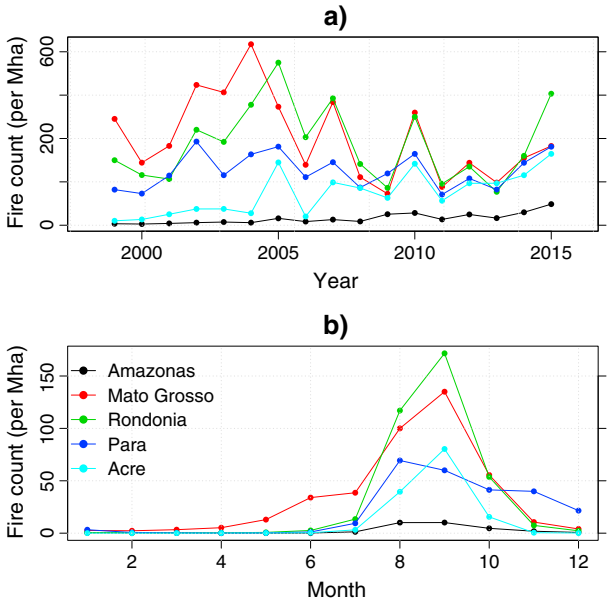

Figure 4. (a) Annual total fire count (per Mha). (b) Seasonal cycle of fire count (per Mha).

for both variables. The Pearson correlation coefficients are 0.74 and −0.63, respectively, for temperature and precipitation. Both values are statistically significant at the 5% significance level (p value $< 2.2 \cdot 10^{-16}$). The Spearman correlation coefficients, which are more appropriate for measuring the magnitude of nonlinear relationships, are 0.78 and −0.81, respectively.

4.3. Poisson Modeling

The response of monthly fire count (per Mha) across the Brazilian Amazon for concurrent variations in temperature and rainfall as predicted by the benchmark model proposed above (equation (5)) is shown in Figure 6. The model is fit considering the 1998–2013 overlapping period of predictors (rainfall and temperature) and the response variable (fire count). A well-defined boundary for temperature below around 31.5°C and for rainfall above 220 mm/month defines a region in which the fire count is less than nine active fires per Mha. For rainfall less than 150 mm/month, the temperature plays a more significant role, since contour lines are closer to horizontal lines, where rainfall has no effect. The number of fires increases considerably for temperature above 34°C and rainfall below 100 mm/month. The results individualized by states have similar patterns (not shown here). The Poisson R^2 measure for this model as defined in equation (15) is 0.7865, meaning that the model that incorporates the concurrent temperature and rainfall explains around 78% of the deviance of a model based solely on the mean value of the fire counts (null model). Despite the relatively high correlation between rainfall and temperature (Figure 3), the variance inflation factor (see Fox, 2008) for the benchmark model is 1.63, indicating only moderate levels of multicollinearity.

The expected fire rates as predicted by the benchmark model in Figure (6) can be easily converted into conditional probabilities for the active fire counts, leading to a better interpretation of the impacts of temperature on fires after accounting for rainfall. For instance, Figure 7 shows prediction of the expected fire count as a function of temperature above the September average value (33.9°C) and conditional on a fixed rainfall equal to the average value for September (104 mm/month), which is the peak season for fires (Figure 4). The relation is close to linear, and we observe that within the range of historical, average daily maximum temperatures for September (33.9°C–34.8°C), there is an increase in the predicted rate from 57 to 73 fires (per Mha), which is about 19 fires (per Mha) per degree Celsius increase in temperature. The changes in the likelihood of fires associated with the changes in the expected fire count are illustrated in Figure 7 (right). A remarkable shift in the exceedance probabilities can be seen in response to changes in temperature. For example, the probability of active fires to exceed the median number for September (55) goes from 57% for $T = 33.9$°C to 98% for $T = 34.8$°C.

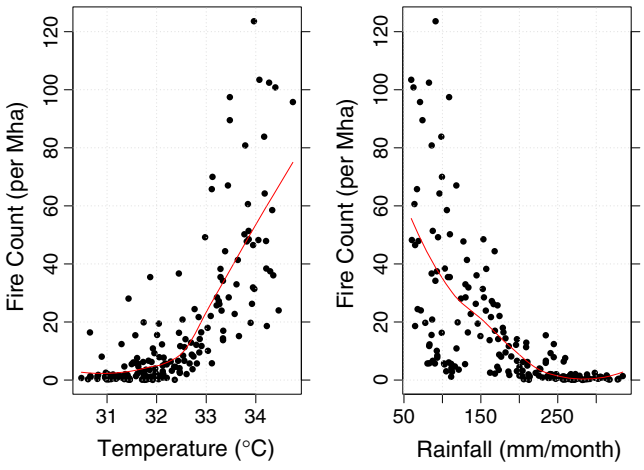

Figure 5. Relation of monthly fire count (per Mha) over the Amazon and (left) temperature and (right) rainfall.

The Poisson R^2 measure for different model combinations, including the past month fire count, is shown in Table 1 for the entire Amazon and for each one of the states. Considering the concurrent variables, the temperature leads to higher R^2 values for the whole Amazon and all states but Mato Grosso. The temperature has the largest effect on fire counts for the states of Para, Acre, and Rondônia. After accounting for rainfall, temperature (comparison of model $P_t\ T_t$ with model P_t) raises the R^2 measure by values between 8% and 30%. On the other hand, the effect of rainfall after accounting for temperature (comparison of model $P_t\ T_t$ with model T_t) has a minor role, increasing less than 10% for all states but Mato Grosso, where it adds 21% for R^2.

The previous month fire count, which could be an indicative of fuel moisture status, plays also a significant role on explaining the fire counts. Alone (model F_{t-1}), it explains around 55%–65% of the data deviance. After accounting for the previous fire count, the role of temperature (compare models $T_t\ F_{t-1}$, and F_{t-1}) diminishes when compared with the role of rainfall (compare models $P_t\ F_{t-1}$, and F_{t-1}). The temperature in this case raises R^2 by 6%–30%, while rainfall increases by 20%–35%. This may reflect the greater effect of temperature

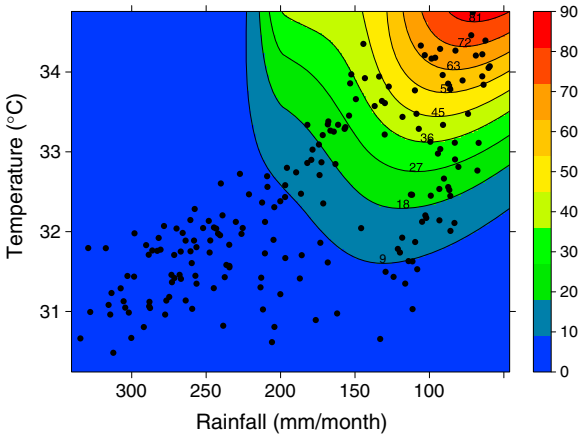

Figure 6. Predictions of average monthly fire count (per Mha) over the Brazilian Amazon as a function of monthly temperature (average of daily maximum) and total rainfall. The black dots show observed values.

on fire count and the persistence of temperature, since F_{t-1} is highly correlated with the concurrent temperature (T_{t-1}) and there is a high persistence of temperature (high correlation of T_{t-1} and T_t), so that by adding F_{t-1} in the model we basically remove the marginal gains obtained by including T_t in the model. The three variables together explain over 88% of the fire count variability.

4.4. Effect of Past Temperature, Rainfall, and Fire Count

The effect of past temperature, rainfall, and fire count on the current active fires is evaluated by analyzing the R^2 (equation (15)) measure as estimated by adding past values of each one of these variables to the null model, which contains only the intercept term. The results are shown in Figure 8 (blue bars). All three covariates lead to models with considerable values of R^2, with a general tendency of smaller values between the lags of 3–4 months and values as high as 60% for lag times between 5 and 6 months.

The conditional effect of past temperature, rainfall, and fire count is evaluated by the R^2 measure (equation (18)) estimated by adding past values of these variables to the benchmark model, which now has temperature T_t and rainfall P_t as predictors. After accounting for the concurrent temperature and rainfall, the marginal gain in extra deviance explained by past values is drastically reduced for all three variables (red bars in Figure 8) when compared with the marginal gains obtained by adding these variables to the null model (blue bars in Figure 8). The marginal gain is less than 10% for rainfall and temperature and 14% for the fire count at lag equal to 1 month. Similar results are obtained for each state individually (not shown here).

5. Summary and Conclusions

The active fire counts in the Brazilian Amazon were modeled in this work as a function of maximum daily temperature and daily rainfall. A Poisson regression model was used to model the expected frequency of monthly fire count in the Brazilian Amazon as a function of the average (over months) maximum daily temperature and monthly total rainfall depth. Both predictor variables were spatially averaged over the Amazon region. A local regression model (locfit) was employed to allow nonlinearities between the mean response (after the appropriate transformation through the link function) and the covariates. The model was fit to the fire count series for each Brazilian state within the Amazon (Acre, Amazonas, Mato Grosso, Pará, and Rondônia) as well as to the aggregate values for the entire region.

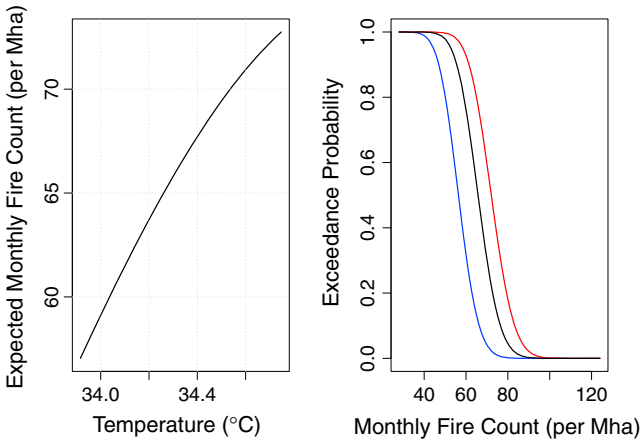

Figure 7. (left) Expected monthly fire count for the Brazilian Amazon (in Mha) as predicted by the benchmark model for the average rainfall of September (104 mm/month). (right) Exceedance probabilities obtained from a Poisson distribution with average fire rates as predicted in Figure 7 (left) for three different values of temperature: 33.9°C (blue line), 34.3°C (black line), and 34.8°C (red line).

A significant, increasing monotonic trend was observed for the maximum daily temperature, with no correspondent trend in rainfall. Both variables are strongly negatively correlated when we analyzed the raw data as well as anomalies after removing the seasonal cycle. The correlation peaks at zero lag, suggesting that years of low rainfall are accompanied by high temperatures due to the same causing mechanism rather than regional feedbacks from the vegetation in response to the low rainfall. The time of the year of the lowest rainfall and highest temperature (August–September) coincides with the fire peak season.

When modeling the fire count over the whole Amazon as a function of the concurrent temperature and rainfall, we observed that the fire counts are relatively low (less than 9 per month per Mha) for temperatures below 31.5° C and rainfall above 220 mm/month. The number increases for temperatures above and rainfalls below these threshold values. Considering the average rainfall for September (fire peak month), the model suggests that for a 1°C increase in the monthly average of maximum daily temperatures, the number of fire counts increases by 19 fires per Mha (or 30% above the average value of 64 actives fires per Mha for September). Such changes in the expected number of active fires yield major changes in the likelihood of fires as seen in the exceedance probability curves. The sensitivity of fire counts to a 1°C increase

Table 1
R^2 Measure (in Percent) for Different Poisson Regression Models for the Fire Counts in the Amazon

	Region					
Model	The entire Amazon	Amazonas	Mato Grosso	Rondônia	Para	Acre
P_t	61.1	51.8	63.8	57.8	44.3	53.4
T_t	71.4	68.6	50.7	74.6	71.9	70.6
F_{t-1}	60.1	54.3	65.2	62.8	55.5	58.4
P_t T_t	78.6	73.7	71.1	83.1	74.9	79.3
P_t F_{t-1}	90.5	89.8	85.4	92.7	87.2	92.7
T_t F_{t-1}	78.9	76.6	71.2	81.7	84.4	80.1
P_t T_t F_{t-1}	92.5	91.2	88.5	93.9	88.6	93.0

in temperatures highlights the vulnerability of the Amazon region in a warming climate where much higher temperatures are expected by the end of this century.

The Poisson model results indicate a strong role of temperature on fire counts in the Amazon, which has not been fully explored in the literature. About 68% of the deviance in fire counts is explained by the concurrent temperature-fire information (here, temperature refers to the monthly average of the daily maximum temperatures). This finding holds for all states but Mato Grosso. The concurrent rainfall-fire count information explains on average 55% of the fire count deviance and can be as low as 44% for the state of Pará. After accounting for the temperature-fire relationship, rainfall explains additional 9% of the fire count deviance whereas, after accounting for rainfall-fire relationship, temperature explains additional 21% of the fire count deviance. This provides evidence for a stronger control on active fires by temperature than precipitation. The fire count of previous month, which may be a proxy for fuel moisture content, also has a significant role and explains, on average, additional 19% of the fire count deviance after considering the concurrent temperature-rainfall information. Together, all these three variables explain on average 91% of the fire count

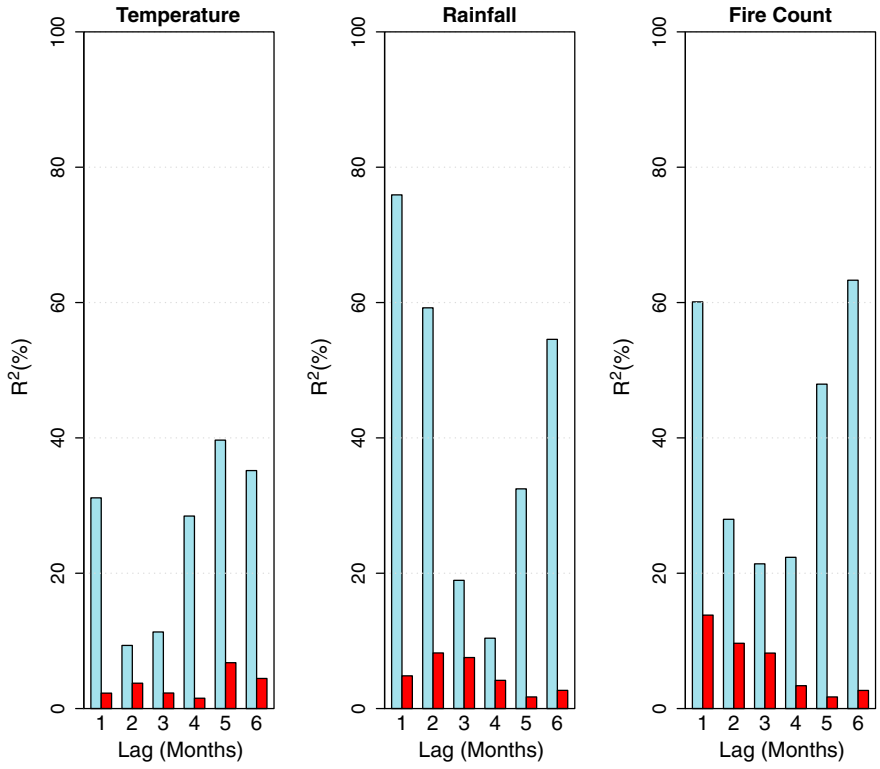

Figure 8. R^2 measure estimated by adding the past variables (left) temperature, (middle) rainfall, and (right) fire count to the null model (blue bars) and to the benchmark model (red bars).

variability. More generally, as a consequence of the high correlation of rainfall and temperature, around 55% of the fire count deviance can be explained by either rainfall or temperature or the combination of these variables, although the individual effects cannot be distinguished under the model proposed in this work.

Antecedent rainfall and temperature seem to play a minor direct influence on the fire count data relative to concurrent rainfall-temperature-fire information. After accounting for the concurrent values of rainfall-temperature, the effect of antecedent rainfall and temperature as per the R^2 measure drops significantly. This suggests that the major impacts of rainfall and temperature on the fire counts through direct (through rainfall) and indirect effects (through evapotranspiration) on the deep soil water content and relative humidity are limited to 1 to 3 months ahead. Strong correlations found between fire count data and antecedent (beyond 4 months lag times) rainfall and temperature might be more related to the temporal persistence of rainfall and temperature rather than any direct effect of them on the forest flammability. The previous time series history of active fires was also found to play a major role, possibly because it could be a proxy for the deep soil water content of previous month and consequently act as an almost independent predictor for the relative humidity and fire count of the following month.

Finally, these results indicate that the impact of temperature on the Amazon flammability can be at least as significant as (but probably greater) that of rainfall, especially at short time scale (1–3 months). As a result, the effects of global warming on Amazon fires may be stronger than what has been estimated in previous studies. There is less uncertainty in the projected increase in the temperature over the Amazon when compared with the uncertainties in future rainfall. Historical data show no trend in rainfall, at least when spatially averaged across the region, and if this scenario persists in the future, then the number of fires should increase significantly due to the overpressure on the deep groundwater caused by an increasing evaporation in response to higher temperatures and no corresponding increase in rainfall.

Acknowledgments
Satellite active fire observations for the Brazilian states within the Amazon region are provided by the Brazilian National Institute of Space Research (INPE) and can be obtained at https://queimadas.dgi.inpe.br/queimadas/portal. The rainfall and temperature data are provided by Xavier et al. (2016) and can be accessed at http://careyking.com/data-download/. The first author acknowledges a Postdoctoral Fellowship from the Brazilian Government Agency CNPq (Conselho Nacional de Desenvolvimento Cientifico e Tecnologico) during part of this work. The second author was partially supported by the National Aeronautics and Space Administration (NASA) award NNX15AC27G and National Oceanic and Atmospheric Administration (NOAA) award NA14OAR4310222.

References

Aghakouchak, A., Cheng, L., Mazdiyasni, O., & Farahmand, A. (2014). Global warming and changes in risk of concurrent climate extremes: Insights from the 2014 California drought. *Geophysical Research Letters*, *41*, 8847–8852. https://doi.org/10.1002/2014GL062308

Alencar, A., Nepstad, D., & Diaz, M. C. V. (2006). Forest understory fire in the Brazilian Amazon in ENSO and non-ENSO years: Area burned and committed carbon emissions. *Earth Interactions*, *10*(6), 1–17. https://doi.org/10.1175/EI150.1

Aragão, L. E. O. C., Malhi, Y., Roman-Cuesta, R. M., Saatchi, S., Anderson, L. O., & Shimabukuro, Y. E. (2007). Spatial patterns and fire response of recent Amazonian droughts. *Geophysical Research Letters*, *34*, L07701. https://doi.org/10.1029/2006GL028946

Aragão, L. E. O. C., & Shimabukuro, Y. E. (2010). The incidence of fire in Amazonian forests with implications for REDD. *Science*, *328*(5983), 1275–1278.

Artaxo, P., Rizzo, L. V., Brito, J. F., Barbosa, H. M. J., Arana, A., Sena, E. T., … Andreae, M. O. (2013). Atmospheric aerosols in Amazonia and land use change: From natural biogenic to biomass burning conditions. *Faraday Discussions*, *165*, 203–235. https://doi.org/10.1039/C3FD00052D

Badger, A. M., & Dirmeyer, P. A. (2016). Remote tropical and sub-tropical responses to Amazon deforestation. *Climate Dynamics*, *46*(9), 3057–3066. https://doi.org/10.1007/s00382-015-2752-5

Brown, I. F., Schroeder, W., Setzer, A., De Los Rios Maldonado, M., Pantoja, N., Duarte, A., & Marengo, J. (2006). Monitoring fires in southwestern Amazonia rain forests. *Eos, Transactions American Geophysical Union*, *87*(26), 253–259. https://doi.org/10.1029/2006EO260001

Cameron, A. C., & Windmeijer, F. A. G. (1996). R-Squared measures for count data regression models with applications to health-care utilization. *Journal of Business & Economic Statistics*, *14*(2), 209–220. https://doi.org/10.2307/1392433

Cardoso, M. F., Hurtt, G. C., Moore, B., Nobre, C. A., & Prins, E. M. (2003). Projecting future fire activity in Amazonia. *Global Change Biology*, *9*(5), 656–669. https://doi.org/10.1046/j.1365-2486.2003.00607.x

Chen, Y., Morton, D. C., Jin, Y., Collatz, G. J., Kasibhatla, P. S., van der Werf, G. R., … Randerson, J. T. (2013). Long-term trends and interannual variability of forest, savanna and agricultural fires in South America. *Carbon Management*, *4*(6), 617–638. https://doi.org/10.4155/cmt.13.61

Chen, Y., Randerson, J. T., Morton, D. C., DeFries, R. S., Collatz, G. J., Kasibhatla, P. S., … Marlier, M. E. (2011). Forecasting fire season severity in South America using sea surface temperature anomalies. *Science*, *334*(6057), 787–791. https://doi.org/10.1126/science.1209472

Cochrane, M. A. (2003). Fire science for rainforests. *Nature*, *421*, 913–919. https://doi.org/10.1038/nature01437

Cochrane, M. A., & Barber, C. P. (2009). Climate change, human land use and future fires in the Amazon. *Global Change Biology*, *15*(3), 601–612. https://doi.org/10.1111/j.1365-2486.2008.01786.x

Cochrane, M. A., Alencar, A., Schulze, M. D., Souza, C. M., Nepstad, D. C., Lefebvre, P., & Davidson, E. A. (1999). Positive feedbacks in the fire dynamic of closed canopy tropical forests. *Science*, *284*(5421), 1832–1835. https://doi.org/10.1126/science.284.5421.1832

de Linage, C., Famiglietti, J. S., & Randerson, J. T. (2014). Statistical prediction of terrestrial water storage changes in the Amazon Basin using tropical Pacific and North Atlantic sea surface temperature anomalies. *Hydrology and Earth System Sciences*, *18*, 2089–2102.

Debortoli, N. S., Dubreuil, V., Funatsu, B., Delahaye, F., de Oliveira, C. H., Rodrigues-Filho, S., … Fetter, R. (2015). Rainfall patterns in the Southern Amazon: A chronological perspective (1971–2010). *Climatic Change*, *132*(2), 251–264. https://doi.org/10.1007/s10584-015-1415-1

Drumond, A., Nieto, R., Gimeno, L., & Ambrizzi, T. (2008). A Lagrangian identification of major sources of moisture over central Brazil and La Plata Basin. *Journal of Geophysical Research*, *113*, D14128. https://doi.org/10.1029/2007JD009547

Fernandes, K., Baethgen, W., Bernardes, S., DeFries, R., DeWitt, D. G., Goddard, L., … Uriarte, M. (2011). North tropical Atlantic influence on western Amazon fire season variability. *Geophysical Research Letters*, *38*, L12701. https://doi.org/10.1029/2011GL047392

Fernandes, K., Giannini, A., Verchot, L., Baethgen, W., & Pinedo-Vasquez, M. (2015). Decadal covariability of Atlantic SSTs and western Amazon dry-season hydroclimate in observations and CMIP5 simulations. *Geophysical Research Letters*, *42*, 6793–6801. https://doi.org/10.1002/2015GL063911

Fox, J. (2008). *Applied regression analysis and generalized linear models* (2nd ed., 688 pp.). Thousand Oaks: SAGE Publications Inc.
Gatti, L. V., Gloor, M., Miller, J. B., Doughty, C. E., Malhi, Y., Domingues, L. G., … Lloyd, J. (2014). Drought sensitivity of Amazonian carbon balance revealed by atmospheric measurements. *Nature*, *506*, 76–80. https://doi.org/10.1038/nature12957
Gloor, M., Barichivich, J., Ziv, G., Brienen, R., Schöngart, J., Peylin, P., … Baker, J. (2015). Recent Amazon climate as background for possible ongoing and future changes of Amazon humid forests. *Global Biogeochemical Cycles*, *29*, 1384–1399. https://doi.org/10.1002/2014GB005080
Golding, N., & Betts, R. (2008). Fire risk in Amazonia due to climate change in the HadCM3 climate model: Potential interactions with deforestation. *Global Biogeochemical Cycles*, *22*, GB4007. https://doi.org/10.1029/2007GB003166
Hao, Z., AghaKouchak, A., & Phillips, T. (2013). Changes in concurrent monthly precipitation and temperature extremes. *Environmental Research Letters*, *8*(3), 034014. https://doi.org/10.1088/1748-9326/8/3/034014
Laurance, W. F., & Williamson, G. B. (2001). Positive feedbacks among forest fragmentation, drought, and climate change in the Amazon. *Conservation Biology*, *15*(6), 1529–1535. https://doi.org/10.1046/j.1523-1739.2001.01093.x
Liu, Y., Stanturf, J., & Goodrick, S. (2010). Trends in global wildfire potential in a changing climate. *Forest Ecology and Management*, *259*(4), 685–697. https://doi.org/10.1016/j.foreco.2009.09.002
Loader, C. (1999). *Local regression and likelihood*. New York: Springer.
Loader, C. (2013). locfit: Local regression, likelihood and density estimation., R package version 1.5-9.1.
Malhi, Y., & Wright, J. (2004). Spatial patterns and recent trends in the climate of tropical rainforest regions. *Philosophical Transactions of the Royal Society of London B: Biological Sciences*, *359*(1443), 311–329. https://doi.org/10.1098/rstb.2003.1433
Marengo, J. A., & Espinoza, J. C. (2016). Extreme seasonal droughts and floods in Amazonia: Causes, trends and impacts. *International Journal of Climatology*, *36*, 1033–1050.
Marengo, J. A., Nobre, C. A., Tomasella, J., Oyama, M. D., De Oliveira, G. S., De Oliveira, R., … Brown, I. F. (2008). The drought of Amazonia in 2005. *Journal of Climate*, *21*(3), 495–516. https://doi.org/10.1175/2007JCLI1600.1
Marengo, J. A., Tomasella, J., Alves, L. M., Soares, W. R., & Rodriguez, D. A. (2011). The drought of 2010 in the context of historical droughts in the Amazon region. *Geophysical Research Letters*, *38*, L12703. https://doi.org/10.1029/2011GL047436
Mazdiyasni, O., & AghaKouchak, A. (2015). Recognize anthropogenic drought. *Proceedings of the National Academy of Sciences of the United States of America*, *112*(35), 1–6. https://doi.org/10.1073/pnas.1422945112
McClain, M. E., Victoria, R., & Richey, J. E. (2001). *The biogeochemistry of the Amazon Basin* (384 pp.). Oxford, UK: Oxford University Press.
McCullagh, P., & Nelder, J. A. (1989). *Generalized linear models* (2nd ed., 532 pp.). Boca Raton, FL: Chapman and Hall/CRC.
Nepstad, D., Lefebvre, P., Lopes da Silva, U., Tomasella, J., Schlesinger, P., Solórzano, L., … Guerreira Benito, J. (2004). Amazon drought and its implications for forest flammability and tree growth: A basin-wide analysis. *Global Change Biology*, *10*, 704–717. https://doi.org/10.1111/j.1529-8817.2003.00772.x
Nepstad, D. C., Moreira, A. G., & Alencar, A. (1999). Flames in the rain forest: Origins, impacts and alternatives to Amazonian fire (Tech. Rep.). Brasilia, Brazil: World Bank.
Nobre, C. A., Sellers, P. J., & Shukla, J. (1991). Amazonian deforestation and regional climate change. *Journal of Climate*, *4*(10), 957–988. https://doi.org/10.1175/1520-0442(1991)004<0957:ADARCC>2.0.CO;2
Phillips, O. L., Aragão, L. E. O. C., Lewis, S. L., Fisher, J. B., Lloyd, J., López-González, G., & Torres-Lezama, A. (2009). Drought sensitivity of the Amazon rainforest. *Science*, *323*(5919), 1344–1347. https://doi.org/10.1126/science.1164033
Rao, V. B., Franchito, S. H., Santo, C. M. E., & Gan, M. A. (2016). An update on the rainfall characteristics of Brazil: Seasonal variations and trends in 1979–2011. *International Journal of Climatology*, *36*(1), 291–302. https://doi.org/10.1002/joc.4345
Ray, D., Nepstad, D., & Moutinho, P. (2005). Micrometeorological and canopy controls of fire susceptibility in a forested Amazon landscape. *Ecological Applications*, *15*(5), 1664–1678. https://doi.org/10.1890/05-0404
Roman-Cuesta, R. M., Rejalaga-Noguera, L., Pinto-García, C., & Retana, J. (2014). Pacific and Atlantic oceanic anomalies and their interaction with rainfall and fire in Bolivian biomes for the period 1992–2012. *Climatic Change*, *127*, 243–256. https://doi.org/10.1007/s10584-014-1246-5
Ropelewski, C., & Halpert, M. (1987). Global and regional scale precipitation patterns associated with the El Niño/Southern Oscillation. *Monthly Weather Review*, *115*, 1606–1626.
Shukla, S., Safeeq, M., AghaKouchak, A., Guan, K., & Funk, C. (2015). Temperature impacts on the water year 2014 drought in California. *Geophysical Research Letters*, *42*, 4384–4393. https://doi.org/10.1002/2015GL063666
Silvestrini, R. A., Soares-Filho, B. S., Nepstad, D., Coe, M., Rodrigues, H., & Assunção, R. (2011). Simulating fire regimes in the Amazon in response to climate change and deforestation. *Ecological Applications*, *21*(5), 1573–1590. https://doi.org/10.1890/10-0827.1
Sun, Q., Miao, C., AghaKouchak, A., & Duan, Q. (2016). Century-scale causal relationships between global dry/wet conditions and the state of the Pacific and Atlantic Oceans. *Geophysical Research Letters*, *43*, 6528–6537. https://doi.org/10.1002/2016GL069628
Swain, D. L., Tsiang, M., Haugen, M., Singh, D., Charland, A., Rajaratnam, B., & Diffenbaugh, N. S. (2014). The extraordinary California drought of 2013/2014: Character, context, and the role of climate change. *Bulletin of the American Meteorological Society*, *95*(9), 3–7.
Turco, M., von Hardenberg, J., AghaKouchak, A., Llasat, M. C., Provenzale, A., & Trigo, R. M. (2017). On the key role of droughts in the dynamics of summer fires in Mediterranean Europe. *Scientific Reports*, *7*, 81.
Uhl, C., & Kauffman, J. B. (1990). Deforestation, fire susceptibility, and potential tree responses to fire in the eastern Amazon. *Ecology*, *71*(2), 437–449.
van der Werf, G. R., Randerson, J. T., Giglio, L., Gobron, N., & Dolman, A. J. (2008). Climate controls on the variability of fires in the tropics and subtropics. *Global Biogeochemical Cycles*, *22*, GB3028. https://doi.org/10.1029/2007GB003122
Veldman, J. W., & Putz, F. E. (2011). Grass-dominated vegetation, not species-diverse natural savanna, replaces degraded tropical forests on the southern edge of the Amazon Basin. *Biological Conservation*, *144*(5), 1419–1429. https://doi.org/10.1016/j.biocon.2011.01.011
Xavier, A. C., King, C. W., & Scanlonc, B. R. (2016). Daily gridded meteorological variables in Brazil (1980–2013). *International Journal of Climatology*, *36*, 2644–2659.
Yoon, J.-H., & Zeng, N. (2010). An Atlantic influence on Amazon rainfall. *Climate Dynamics*, *34*(2), 249–264. https://doi.org/10.1007/s00382-009-0551-6